Electric Power Systems Research 120 (2015) 177–183

Contents lists available at ScienceDirect

Electric Power Systems Research

journal homepage: www.elsevier.com/locate/epsr

Implementation of autonomous distributed V2G to electric vehicle and DC charging system

Yutaka Ota*, Haruhito Taniguchi, Jumpei Baba, Akihiko Yokoyama

The University of Tokyo, Japan

ARTICLE INFO

Article history:
Received 1 February 2014
Received in revised form 9 May 2014
Accepted 23 May 2014
Available online 13 June 2014

Keywords:
Electric vehicle
Vehicle-to-Grid
Scheduled charging
DC charging system
Fast demand response
Battery management

ABSTRACT

Vehicle-to-Grid (V2G) has potential for providing the distributed spinning reserve to the power system. We proposed an autonomous V2G control scheme managing the vehicle user's convenience, the battery condition during the idle time, and the contribution to the power system, simultaneously. V2G power is controlled corresponding to the frequency deviation detected at the plug-in terminal and the desirable battery State-of-Charge for the plug-out. In this paper, the proposed control scheme is implemented to an electric vehicle and charging system. Performances of the interface, communication and control structure, and system efficiency and time response are verified by using the test system coordinating an electric vehicle battery test bed with a DC charging port, a controllable bi-directional power conditioner, and an integrated interface controller.

1. Introduction

Electric vehicle (EV) is a possible candidate of demand response resource because of equipping the EV with the high performance battery energy storage. Smart charging schemes considering the power system operating conditions have been proposed [1–4]. Vehicle-to-Grid (V2G) brings an additional value to the ancillary services of the power system [5]. Potential analyses and some control strategies of the V2G have been discussed [6–9]. We also proposed an integrated load frequency control (LFC) scheme consisted with an autonomous distributed V2G [10] and an aggregation strategy of the multiple EVs [11].

Toward the actual implementation of the V2G to the EV and the charging system, the V2G capable motor inverter [5], on-board charger [12–14], and off-board charger [15] have so far been investigated. Among them, this paper is focusing on the off-board charger because the vehicle-grid interface is already established for the quick charging application to few commercial EVs. It is still not considered that seamless and quick control of the bi-directional power flow to meet sudden grid frequency change and integration of the off-board charger and automotive components for the V2G.

In this paper, the autonomous distributed V2G control requiring seamless and quick response is actually implemented to an EV and charging system for a trial. A bi-directional controllable power conditioner is connected with an EV battery test-bed through the DC quick charging port equipped with the commercial EVs. A smart interface controller integrates communication and control of the EV and charging system. System performances are confirmed by fundamental experiments assuming the typical EV usage.

The contents of this paper are as follows. The overall system configuration and specifications of components are described in Section 2. The experimental results are presented in Section 3. Finally, some conclusions are summarized in Section 4.

2. Electric vehicle and charging system

2.1. System structure

Schematic diagram of the EV and charging system, an experimental setup in the laboratory, and the specifications of each component are shown in Figs. 1 and 2, Table 1, respectively. For a safety and indoor experiment, a stationary test-bed is packaged with electrical components of the EV, the battery pack, the battery management unit (BMU), the electric control unit (ECU), and the quick charging inlet. The capacity of the battery is 16 kWh, and maximum charging power for the quick charger is 50 kW. For the household power supply under the power system failure, the V2H (Vehicle-to-Home) system is commercialized targeting the commercial EV with the quick charging port [16]. This research proposes the V2G system that is able to supply 3 kW charge and

---

* Corresponding author at: Eng.Bldg.13-204, 7-3-1, Hongo, Bunkyo-ku, Tokyo 1138656, Japan. Tel.: +81 3 5841 6392; fax: +81 3 5841 6392.
E-mail address: yota@upn.t.u-tokyo.ac.jp (Y. Ota).

http://dx.doi.org/10.1016/j.epsr.2014.05.016

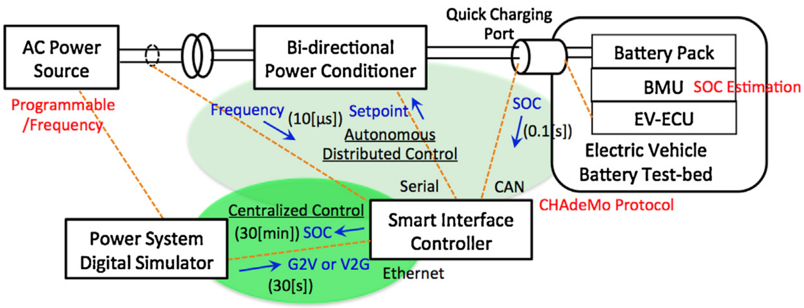

Fig. 1. Schematic diagram of EV and charging system.

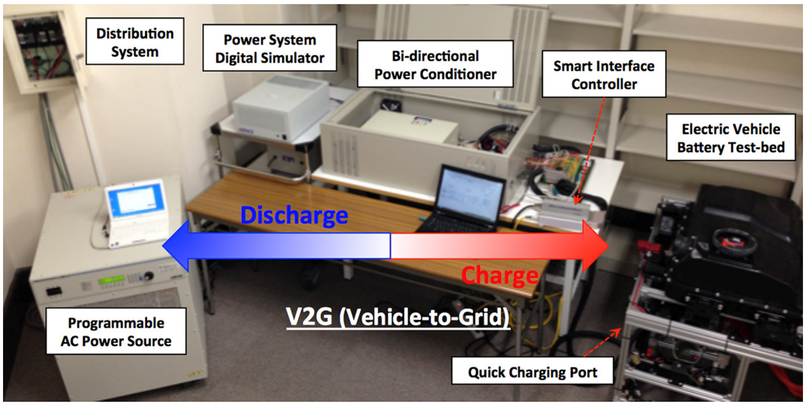

Fig. 2. Experimental setup of EV and charging system.

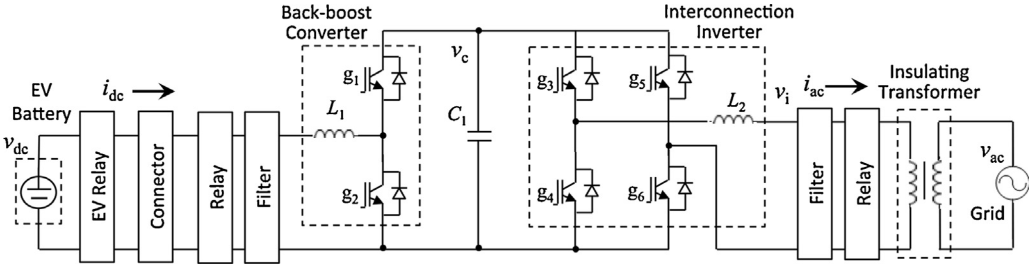

Fig. 3. Electrical circuit of EV and charging system.

Table 1
Specifications of EV and charging system.

Electric vehicle battery test-bed (Mitsubishi Motors i-MiEV)
Battery voltage/capacity: 330 V/16 kWh

Bi-directional power conditioner (Nichikon NECST-TD1)
Maximum power output: 3 kW

Smart interface controller (dSPACE MicroAutoBoxII)
Processor: IBM power PC 750GL 900 MHz
Interface: Serial/CAN/AD/DA/UDP
Control period: 10 µs

Programmable AC power source (California Instruments MX15-1Pi)
Maximum power output (Sync/Source): 15 kVA
Resolution of frequency: 0.01 Hz (accuracy: ±0.01%)

Power system digital simulator (dSPACE DS1006)
Processors: Quad-Core AMD Opteron 2.8 GHz
Interface: Serial/TCP/UDP

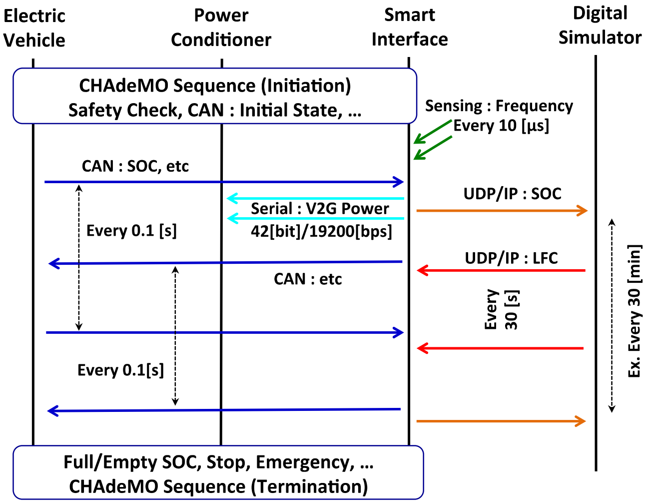

Fig. 4. Time chart of communication and control.

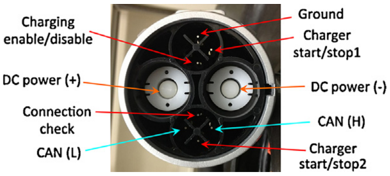

Fig. 5. Pin layout of connector.

discharge power against the power system through the household power outlet.

The smart interface controller communicates with the EV ECU via CAN (Control Area Network) communication, and with the power conditioner via serial communication. The V2G setpoint is determined taking both the system frequency and the battery SOC into account. The system frequency is detected by a precise frequency detection method based on the DFT (Discrete Fourier Transform) [17]. The battery State-of-Charge (SOC) is generally estimated on the EV BMU for the purpose of the EV propulsion control. Therefore, the controller obtains the SOC from the BMU via the CAN communication by use of the CHAdeMO protocol [18], which is designed for the DC quick charging system of the commercial EVs. The V2G power command is transferred to the power conditioner

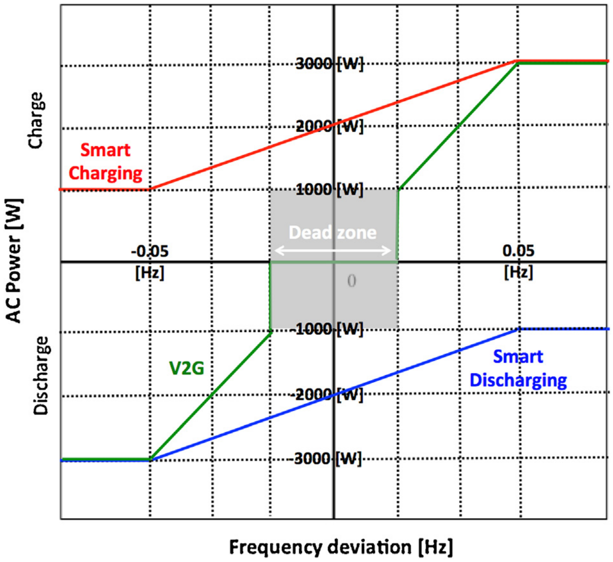

Fig. 6. Control design of autonomous distributed V2G.

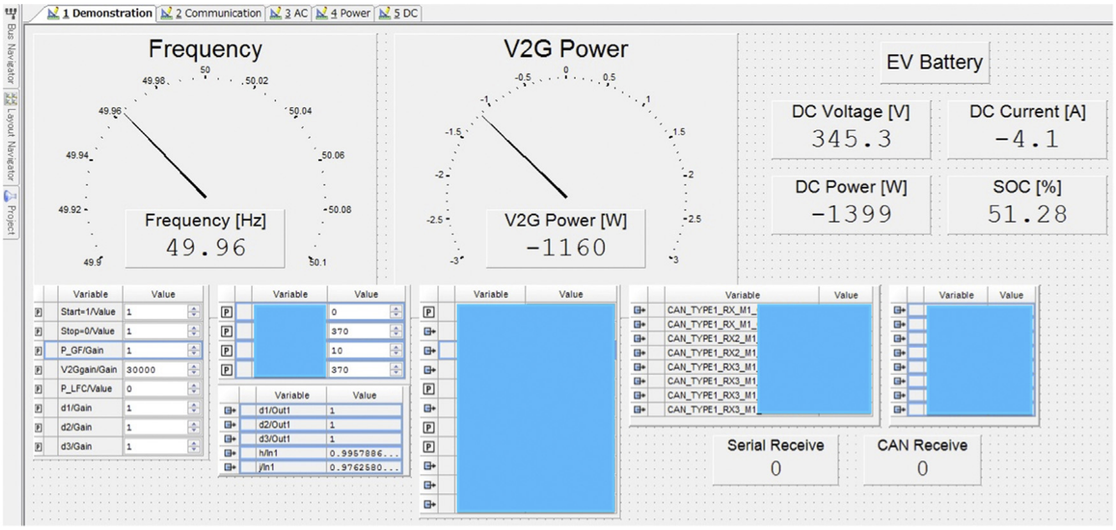

Frequency [Hz]
49.96

V2G Power [W]
-1160

DC Voltage [V]
345.3

DC Current [A]
-4.1

DC Power [W]
-1399

SOC [%]
51.28

Variable	Value
Start=1/Value	1
Stop=0/Value	1
P_GF/Gain	1
V2Ggain/Gain	30000
P_LFC/Value	0
d1/Gain	1
d2/Gain	1
d3/Gain	1

Variable	Value
	0
	370
	10
	370

Variable	Value
d1/Out1	1
d2/Out1	1
d3/Out1	1
h/In1	0.9957886...
j/In1	0.9762580...

Variable	Value
CAN_TYPE1_RX_M1_	
CAN_TYPE1_RX_M1_	
CAN_TYPE1_RX2_M1	
CAN_TYPE1_RX2_M1	
CAN_TYPE1_RX3_M1	
CAN_TYPE1_RX3_M1	
CAN_TYPE1_RX3_M1	
CAN_TYPE1_RX3_M1_	

Serial Receive
0

CAN Receive
0

(a) Grid, vehicle, communicated values

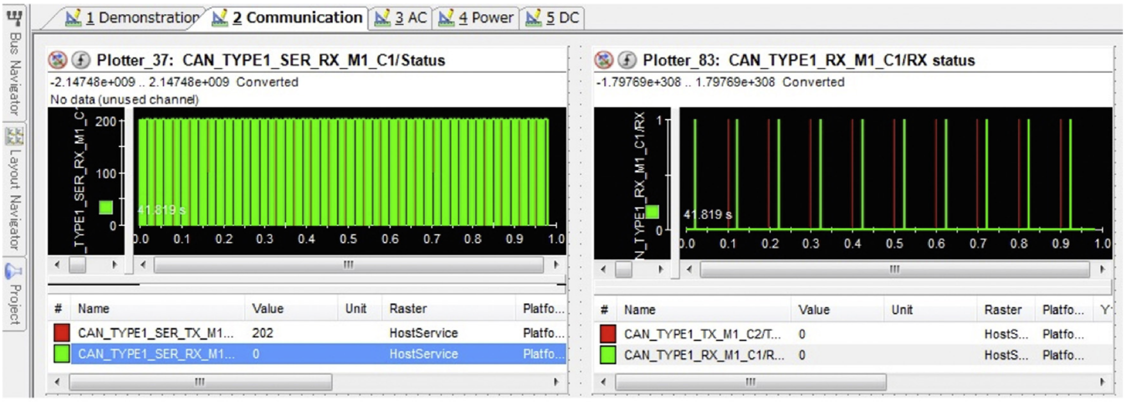

#	Name	Value	Unit	Raster	Platfo...
🟥	CAN_TYPE1_SER_TX_M1...	202		HostService	Platfo...
🟩	CAN_TYPE1_SER_RX_M1...	0		HostService	Platfo...

#	Name	Value	Unit	Raster	Platfo...	Y
🟥	CAN_TYPE1_TX_M1_C2/T...	0		HostS...	Platfo...	
🟩	CAN_TYPE1_RX_M1_C1/R...	0		HostS...	Platfo...	

(b) Communication states

Fig. 7. Operating status of the smart interface controller.

at the right moment by UART (Universal Asynchronous Receiver Transmitter), and then UART receives the send back signal.

The bi-directional power conditioner realizes flexible power flow control in every second. DC 330 V of the vehicle battery is transformed to AC 200 V of the single-phase three-wire distribution system. A typical power electronics circuit is used for the power conversion as shown in Fig. 3. The EV battery is connected to a back-boost converter through an analog filter circuit suppressing ripple components of DC current. An interconnection inverter controls active power for the V2G control and reactive power for the islanding detection.

The system frequency is emulated on the digital simulator with the power system model including renewable energy sources and multiple EVs. Then a programmable AC power source generates an instantaneous voltage of 200 V corresponding to the emulated system frequency. The proposed system supports both the direct interconnection with the actual power system and the interconnection with the emulated power source. A centralized LFC scheme can be carried out considering two-way communication between the smart interface controller and the digital simulator.

2.2. *Communication and control*

Fig. 4 shows a time chart of communication among the components. First of all, initial CHAdeMO sequences are established by checking safety of the EV and the charger. The smart interface controller awakes the EV by an analog signal (Charger start/stop1), and then information exchange is accommodated by the CAN communication. After the compatibility check, the connector lock, the insulation test, and the reclosing of the EV relay are operated by managing three analog signals (Connector check, Charging enable/disable, Charger start/stop2). The pin layout of each line on the connector is shown in Fig. 5. Following the initial sequences, the battery SOC and other operating conditions of the EV and the charger are exchanged every 0.1 s. When the smart interface controller detects termination conditions, CHAdeMO termination sequences are executed.

In the autonomous distributed control, V2G setpoint is determined by droop characteristics in association with the system frequency deviation, shown in Fig. 6 [10]. When user preset plug-out time is approaching, the V2G is switched to the smart charging for satisfying the scheduled charging. In the smart charging, an offset of half of maximum power output is added to the V2G setpoint, and the droop gain is reduced to one-third of that of the V2G. If the SOC is less than 50%, the smart charging is enforced in order to ready for the emergency departure. In this research, the droop gain is set as 600 W/0.01 Hz considering the tradeoff between the control ability and the actual condition of the frequency deviation on the experimental environment. Therefore, maximum charging (discharging) power is supplied for the power system when the system frequency rises (falls) to 50.05 Hz (49.95 Hz). The dead band is also considered to avoid the partial power output conditions, in which the power conversion efficiency is relatively low.

In the centralized control, a load dispatching center need to grasp the battery SOC of each EV with a rough interval, for example, every 30 min. The center selects candidates for the charging (discharging) EVs according to their SOC ascending (descending) order, and then the LFC signals are broadcasted to the selected EVs every thirty seconds. This selective on-off control according to the SOC order is found to be effective for SOC synchronization [11]. The SOC and operating state of each EV is transferred to the digital simulator via UDP/IP communication. If the EV has enough time for the

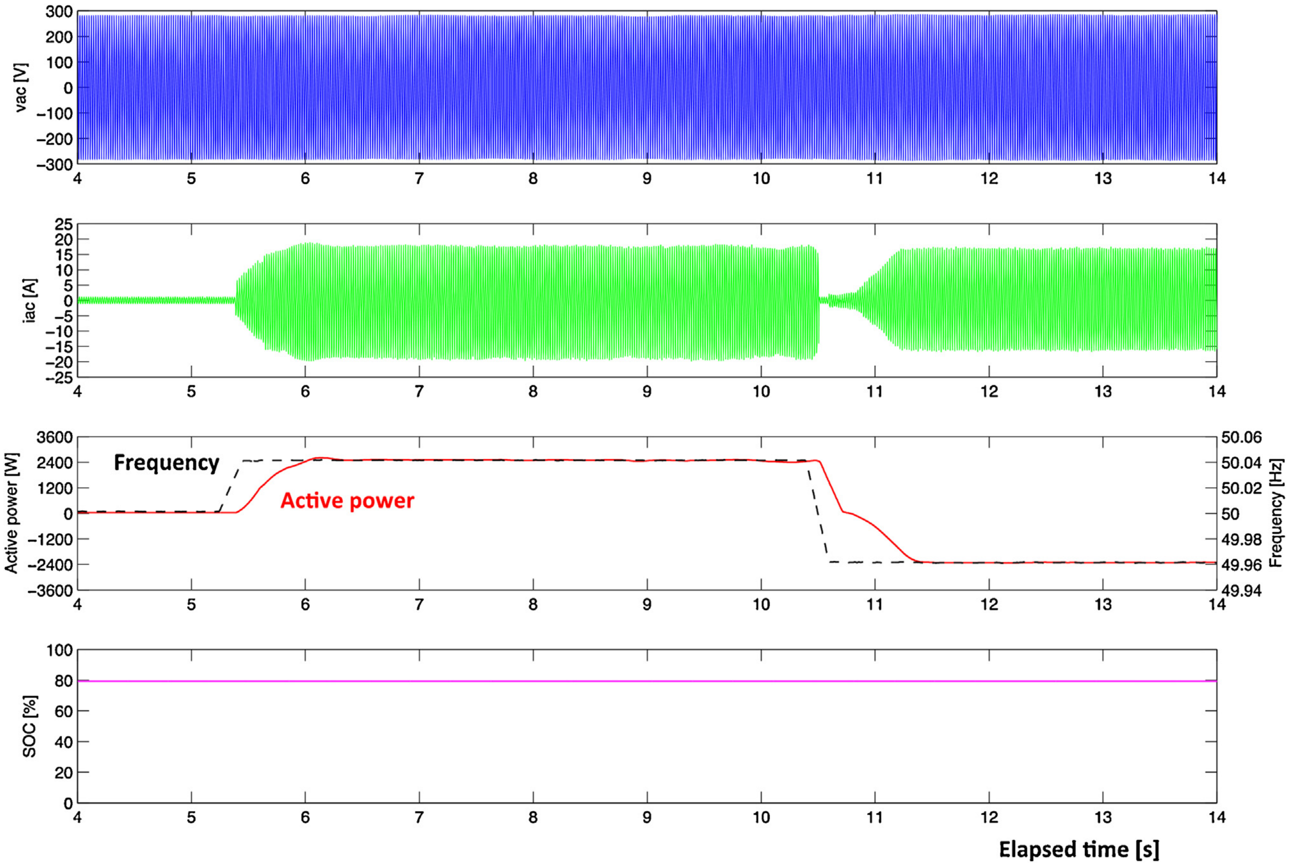

Fig. 8. Experimental results of step response.

user preset plug-out, the EV is ready for receiving the LFC signal from the center. On the other hands, when the emulated LFC signal calculated on the simulator is actually dispatched via the UDP/IP communication, the selected EV switches the V2G to the smart charging (discharging) corresponding to up (down) command in the LFC signal.

2.3. Requirements for smart interface controller

In the proposed system, the smart interface controller plays important role for the system integration. System coordination with HEMS (Home Energy Management System), smart meter, aggregator, utilities, and TSOs/ISOs is also expected for various smart grid applications. Standardized way of communication and control would be required for the actual implementation of the V2G to the worldwide EVs.

In this paper, a rapid prototyping system is adopted in designing the smart interface controller. All the software including communication is described by MATLAB/SIMULINK. Control algorithms, system parameters, communication protocols are flexible, and coordinated operation with the automotive components and the external devices is easily realized. An example of operating status is summarized in Fig. 7.

3. Experimental results

3.1. Step response

First of all, step responses of the system are evaluated under the stepwise frequency change generated by the programmable AC power source. Fig. 8 shows the instantaneous values of AC voltage and AC current, the system frequency, active power output, and the battery SOC received from the EV. The sampling time of the measurements is 1 ms. Specifications of voltage and current sensors and the signal processing are summarized in Table 2. The active power at charge is defined as positive value in this paper.

The frequency change was detected with a 0.2 s delay of the frequency detection method. Then the active power was controlled in response to the detected frequency change with a communication dead time and a delay of the power conversion control. Total settling time was found to be about 1 s. The SOC values were successfully obtained by the CAN communication. The SOC was constant during the experiment because the accumulation of the charge or discharge power, which corresponds to the change of SOC, did not exceed the minimum resolution of the SOC value, which is 0.1 kWh.

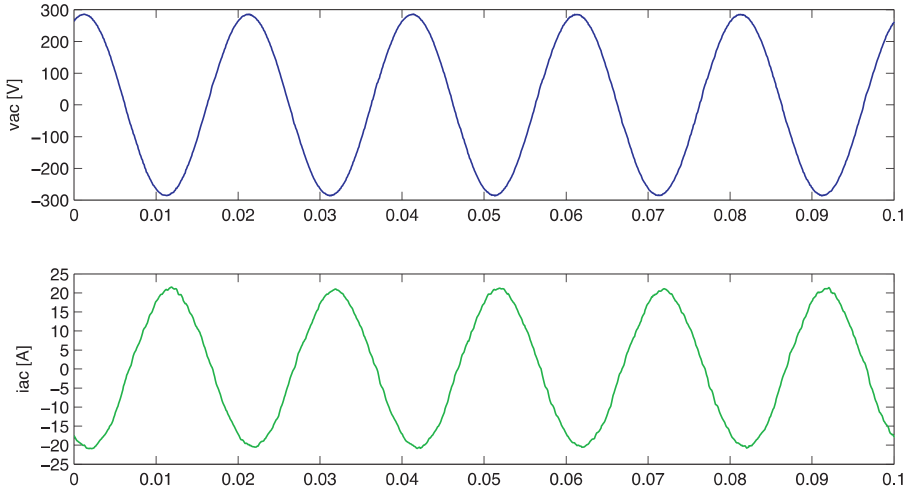

(a) discharge

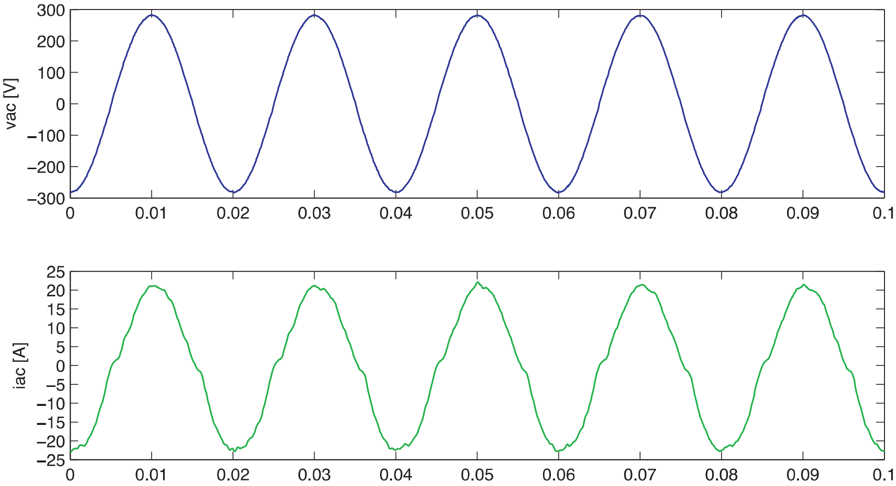

(b) charge

Fig. 9. Instantaneous values of voltage and current.

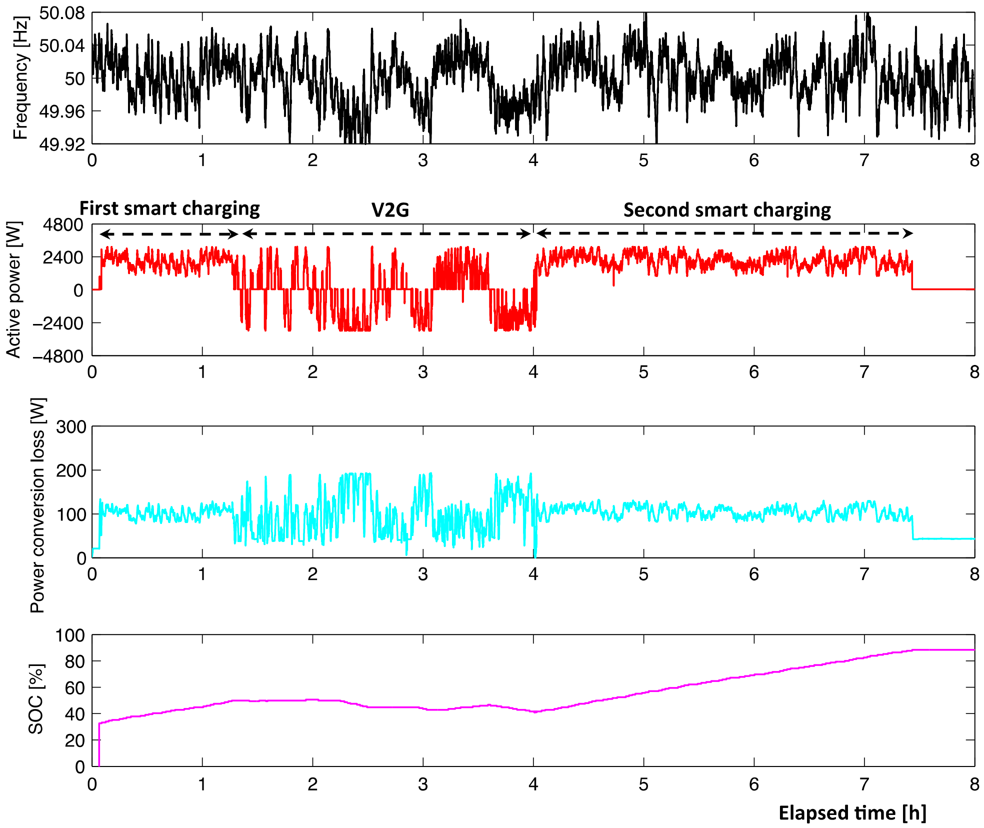

Fig. 10. Experimental results of autonomous distributed V2G.

The instantaneous values of AC voltage and AC current are highlighted in Fig. 9. In this case, the sampling time of the measurements is 0.1 ms. The current phase was properly controlled on the opposite (coordinate) phase against the voltage phase in the discharge (charge) case.

3.2. *Autonomous distributed V2G*

The EV and charging system is directly interconnected with the power system, in which the system frequency fluctuates as a result of the supply and demand imbalance of the actual power system. And the autonomous distributed V2G is verified on the assumption that an EV is plugged-in with 30% SOC, and then plugged-out after seven hours with full charged SOC. Experimental results of the autonomous distributed V2G are shown in Fig. 10. Just after standing up the system, the smart charging was firstly enforced in order to ready for the emergency departure. The EV was charged up to 50% supplying the smart charging with a one-third droop gain against the system frequency deviation. Thereafter the EV continued to supply the charge and discharge cycles by the V2G until about 4 h. Finally, the EV was charged up to the destination SOC (90%) by the second smart charging.

Table 2
Specifications of sensors and signal processing.

AC voltage sensor (M-System M2VF2) Accuracy: ±0.1% of ±300 V Frequency bandwidth: 15 kHz Response time: within 30 μs
DC voltage sensor (M-System M2VF3) Accuracy: ±0.01% of 0–600 V Frequency bandwidth: 12 kHz Response time: within 30 μs
AC current sensor (LEM DHAB S/18) Accuracy: ±0.5% of ±30 A Frequency bandwidth: 1 kHz
DC current sensor (LEM DHAB S/44) Accuracy: ±0.5% of ±20 A Frequency bandwidth: 80 Hz
Signal processing for frequency detection DFT with back-end moving average filter (window width: 0.2 s) [18]
Signal processing for AC and DC power detection Variable window width mean value for instantaneous power (the window width is based on the detected frequency.) and back-end moving average filter (window width: 0.2 s)

Total settling time of the system was within one second including time lags caused by the frequency detection, communication, and response of the power conditioner. So the proposed system was enough to follow the frequency change. The seamless mode switch was also realized in the proposed system. The power conversion loss by the power conditioner was estimated by subtracting the DC power from the AC power. The estimated loss was smoothed by use of the 30 s moving average filter. In the smart charging, the averaged loss was around 100 W. In the V2G, the loss was slightly increased to about 200 W because efficiency at charge was lower than that at discharge in case of the power conditioner used in this research. The power loss in the battery is estimated to be within 10 W by integrating the square of DC current (within 10 A) and the internal resistance of the battery (about 0.1 ohm).

4. Conclusions

In this paper, communication and control interfaces and functions for the V2G is described. Seamless response and high efficient system performance are indispensable for the actual implementation of the autonomous distributed V2G to the EV and charging system. These features were verified by the laboratory test system integrating the commercial EV, the bi-directional power conditioner, and the rapid prototyping controller. Standardization of the connector and the communication protocol for the V2G has been discussed such as the combined charging system with the V2G communication interface [19]. This paper addresses an example of the off-board DC charging system for the V2G.

The autonomous distributed control schemes and the methodology of the system integration are intended to apply the commercial EVs and their charging system. The trial experiences crossing the power and automotive industries by this paper would contribute the actual realization of the V2G technologies to the grid ancillary service and the microgrid operation.

The centralized LFC and further fast demand response schemes are being demonstrated by coordinating remote systems via Ethernet communication. It is expected to realize power & control & communication HILS (Hardware-In-the-Loop Simulation) coupling the power system model, behavior of the multiple EVs, communication characteristics and protocols, and the precise power electronics control all together.

Acknowledgements

This work was supported by CREST from Japan Science and Technology Agency, and Ubiquitous Power Network Endowed Chair of the University of Tokyo. Mitsubishi Motors Corporation supplied an EV battery test-bed. Nichikon Corporation manufactured an order made power conditioner for the V2G. CHAdeMO association instructed about the CHAdeMO protocol. Authors gratefully acknowledge their support.

References

[1] G4V (Grid for Vehicles) [Online]. Available: http://www.g4v.eu
[2] A. Brooks, E. Lu, D. Reicher, C. Spirakis, B. Weihl, Demand dispatch, IEEE Power Eng. Mag. 8 (3) (2010) 20–29.
[3] T. Markel, M. Kuss, J. Foster, D. Manz, M. Mahony, M. Nielsen, A. Reid, D. Richrd, The case for open-source PEV charge management data framework, in: Proc. IEEE International Electric Vehicle Conference, 2012, pp. 1–5.
[4] T. Ikegami, K. Ogimoto, H. Yano, K. Kudo, H. Iguchi, Balancing power supply-demand by controlled charging of numerous electric vehicles, in: Proc. IEEE International Electric Vehicle Conference, 2012, pp. 1–8.
[5] W. Kempton, V. Udo, K. Huber, K. Komara, S. Letendre, S. Baker, D. Brunner, N. Pearre, A Test of Vehicle-to-Grid (V2G) for Energy Storage and Frequency Regulation in the PJM System, Publications of MAGICC (Mid-Atlantic Grid Interface Cars Consortium), 2009.
[6] E. Sortomme, M.A. El-Sharkawi, Optimal combined bidding of Vehicle-to-Grid ancillary services, IEEE Trans. Smart Grid 3 (1) (2012) 70–79.
[7] H. Sekyung, H. Soohee, K. Sezaki, Estimation of achievable power capacity from plug-in electric vehicles for V2G frequency regulation: case studies for market participation, IEEE Trans. Smart Grid 2 (4) (2011) 632–641.
[8] J.A.P. Lopes, F.J. Soares, P.M.R. Almeida, Integration of electric vehicles in the electric power system, Proc. IEEE 99 (1) (2011) 168–183.
[9] M.D. Galus, S. Koch, G. Andersson, Provision of load frequency control by PHEVs, controllable loads, and a cogeneration unit, IEEE Trans. Ind. Electron. 58 (10) (2011) 4568–4582.
[10] Y. Ota, H. Taniguchi, T. Nakajima, K.M. Liyanage, J. Baba, A. Yokoyama, Autonomous distributed V2G (Vehicle-to-Grid) satisfying scheduled charging, IEEE Trans. Smart Grid 3 (1) (2012) 559–564.
[11] K. Shimizu, T. Masuta, Y. Ota, A. Yokoyama, A new load frequency control method in power system using Vehicle-to-Grid system considering users' convenience, in: Proc. Power System Computation Conference, 2011, pp. 1–7.
[12] R.J. Ferreira, L.M. Miranda, R.E. Araujo, J.P. Lopes, A new bi-directional charger for Vehicle-to-Grid integration, in: Proc. IEEE ISGT Europe, 2011, pp. 1–5.
[13] P.B. Anderson, R. Garcia-Valle, W. Kempton, A comparison of electric vehicle integration projects, in: Proc. IEEE PES ISGT Europe, 2012, pp. 1–7.
[14] L. Tang, G. Su, Using onboard electrical propulsion system to provide plug-in charging, V2G and mobile power generation capabilities for HEVs, in: Proc. IEEE Electric Vehicle Conference, 2012, pp. 1–8.
[15] Next Generation EV Charging Infrastructure, Ideal Power Converters White Paper, 2013.
[16] Nichicon Expands EV Charger Lineup with Release of Advanced Function Model V2H System EV Power Station with Remote Controller and Ability to Work with Cogeneration Systems, Nichikon Press Release, 2013.
[17] K. Nakano, Y. Ota, H. Ukai, K. Nakamura, H. Fujita, Frequency detection method based on recursive DFT algorithm, in: Proc. Power Systems Computation Conference, 2002, pp. 1–7.
[18] CHAdeMO Technologies [Online]. Available: http://www.chademo.com/
[19] V2G Interface Specifications between the Electric Vehicle, Local Smart Meter, and ITS Service Providers, Publications of PowerUP, 2012.